

Syntheses, structures and electrochemical properties of single and double helical inorganic complexes containing new polypyridine ligands

Paul Kwok-Keung Ho,^a Shie-Ming Peng,^b Kwok-Yin Wong^a and Chi-Ming Che^{*a}

^a Department of Chemistry, The University of Hong Kong, Pokfulam Road, Hong Kong

^b Department of Chemistry, National Taiwan University, Taipei, Taiwan

New polypyridines [1,3-bis(2,2':6',2''-terpyridin-6-yl)benzene L¹ and 1,3-bis[4-(4-*tert*-butylphenyl)-2,2':6',2''-terpyridin-6-yl]benzene] L² were prepared. Their reactions with copper(II) acetate and silver(I) acetate gave [Cu₂L¹]⁴⁺, [Cu₂L²]⁴⁺, [Ag₂L¹]²⁺ and [Ag₂L²]²⁺ while [Ru₂L²(terpy)₂]⁴⁺ was obtained from [Ru(terpy)Cl₃] (terpy = 2,2':6',2''-terpyridine) with L². The complexes [Cu₂L²][PF₆]₄·6MeCN and [Ag₂L²][PF₆]₂·Me₂CO have been established by X-ray crystal analyses to have double helical structures. Electrospray mass spectrometry showed that the double helical [Cu₂L²]⁴⁺ and [Ag₂L¹]²⁺ complexes and the single helical [Ru₂L²(terpy)₂]⁴⁺ complex are the only species present in solutions. All five complexes undergo reversible oxidations or reductions. Interestingly, the electrochemical data indicate substantial electronic coupling within the bimetallic double helical [M₂L₂]³⁺ (M = Cu or Ag, L = L¹ and L²) but not the single helical [Ru₂L²(terpy)₂]⁴⁺ systems.

The use of 2,2':6',2'':6'':2''':6''':6''''-quinquepyridine¹⁻⁴ and 2,2':6',2'':6'':2''':6''':6''''-sexipyridine⁴⁻⁸ as building blocks for the self-assembly of double helical transition-metal complexes is an area of expanding interest. The bonding character of oligopyridines is manifested in different ways, as three bipyridine units,^{4,5} two terpyridine units⁴⁻⁶ or as a mixture of bipyridine and terpyridine units.^{1,4} The close proximity of these bi- and ter-pyridine units, which is essential to the formation of the double helical complexes, leads to a substantial π - π interaction^{1,4-6} as well as some constraint upon the complex formation.² Many different spacers for linking the oligopyridine units have been used, for example aliphatic ethylene spacers^{9,10} and aromatic 1,3-phenylene spacers.¹¹ These spacers are capable of enhancing the versatility of the compounds in accommodating metal ions with different sizes and different geometries of transition-metal complexes. In addition, the 1,3-phenylene spacer is superior to aliphatic ones due to the lower rotational freedom imposed on the ligands.

Recently, the syntheses of oligopyridines with a 1,3-phenylene spacer and bipyridine units and their metal complexes have been reported by Constable *et al.*¹¹ Herein is described the preparation of a new oligopyridine ligand with a 1,3-phenylene spacer and terpyridine units and its 4-*tert*-butylphenyl derivative, the characterization of double helical silver(I) and copper(II) and single helical ruthenium(II) complexes and their electrochemical properties.

Experimental

Materials

N-[2-Oxo-2-(2,2'-bipyridin-6-yl)ethyl]pyridinium iodide,¹² 1,3-bis(3-dimethylamino-1-oxopropyl)benzene dichloride,¹¹ 4-*tert*-butylbenzaldehyde¹³ and [Ru(terpy)Cl₃]¹⁴ (terpy = 2,2':6',2''-terpyridine) were synthesized according to the literature procedures. 1,3-Diacetylbenzene was obtained from Aldrich, ammonium acetate from Merck, copper(II) acetate from Koch-Light and silver acetate from Fluka. Tetrabutylammonium hexafluorophosphate from Southern Analytical Chemicals, was dried in a vacuum oven at 100 °C for 24 h. Acetonitrile was purified by treatment with KMnO₄ and then distilled over CaH₂. All the other chemicals and solvents were used as received.

Measurements

Proton NMR spectra were recorded on JEOL 270 and DRX-500 Bruker Fourier-transform spectrometers with tetramethylsilane as internal reference. Microanalyses were conducted by Butterworth Laboratories Ltd. The electron impact (EI) mass spectra were recorded on a Finnigan MAT 95 high-resolution mass spectrometer, electrospray mass spectra on the same spectrometer using acetone as mobile phase. Diluted solutions of the compounds were injected directly into the spectrometer *via* a Rheodyne injector. A Harvard Apparatus 20 syringe pump delivered the solution to the vaporization nozzle of the electrospray ion source at a flow rate of 4 μ l min⁻¹. Nitrogen was used as the drying gas, with a flow rate of approximately 3 cm³ s⁻¹. The pressure in the mass analyser region was usually about 10⁻⁸ mbar (10⁻⁶ Pa). About 70–100 signal-averaged spectra were required to give a good signal-to-noise ratio. Cyclic voltammetry was performed with a Princeton Applied Research (PAR) model 175 Universal Programmer and model 173 potentiostat-galvanostat. The working electrode was glassy carbon. Constant-potential coulometry was performed using a PAR model 377A coulometric cell system. The working electrode was a platinum-wire gauze. The solution was stirred with a synchronous stirring motor and under an argon atmosphere during electrolysis. The quantity of electricity passed was measured by a PAR model 179 digital coulometer. All measurements were made against Ag–AgNO₃ (0.1 mol dm⁻³ in MeCN) in acetonitrile with tetrabutylammonium hexafluorophosphate (0.1 mol dm⁻³) as supporting electrolyte.

Syntheses

1,3-Bis(2,2':6',2''-terpyridin-6-yl)benzene L¹. A mixture of *N*-[2-oxo-2-(2,2'-bipyridin-6-yl)ethyl]pyridinium iodide (1.0 g, 2.5 mmol), 1,3-bis(3-dimethylamino-1-oxopropyl)benzene dichloride (0.43 g, 1.25 mmol) and ammonium acetate (4.5 g) in acetic acid (15 cm³) was refluxed for 8 h. The product precipitated after cooling was filtered off and recrystallized twice from toluene to give a white solid (0.25 g, 39%) (Found: C, 79.90; H, 4.30; N, 15.65. Calc, for C₃₆H₂₄N₆: C, 80.00; H, 4.45; N, 15.55%). ¹H NMR (270 Mz, CDCl₃): δ 7.36 (dd, 2 H), 7.69 (t, 1 H), 7.89 (dt, 2 H), 8.00 (m, 6 H), 8.28 (dd, 2 H), 8.49 (d, 2 H), 8.65 (d, 2 H), 8.68 (d, 2 H), 8.74 (d, 2 H), 8.77 (d, 2 H) and

9.00 (s, 1 H). Mass spectrum (EI): m/z 540 (*P*), 462 (*P* – py), and 385 (*P* – 2py).

2,6-Bis(4-*tert*-butylcinnamoyl)benzene. A mixture of 1,3-diacetylbenzene (8.1 g, 30.9 mmol) and 4-*tert*-butylbenzaldehyde (18 cm³) was added to an ice-cooled solution containing sodium hydroxide (5 g), distilled water (50 cm³) and ethanol (30 cm³). The mixture was stirred vigorously until it was so thick that stirring was no longer effective (2–3 h). The reaction mixture was left in an ice-chest for 12 h and then the product was filtered off. It was washed with water and recrystallized from methanol to afford a yellowish crystalline solid (10.6 g, 47%) (Found: C, 85.20; H, 7.40. Calc. for C₃₂H₃₄O₂: C, 85.30; H, 7.60%). ¹H NMR (270 Mz, CDCl₃): δ 1.35 (s, 18 H), 7.54 (dd, 8 H), 7.55 (d, 2 H), 7.65 (t, 1 H), 7.86 (d, 2 H), 8.23 (dd, 2 H), and 8.63 (s, 1 H).

1,3-Bis[4-(4-*tert*-butylphenyl)-2,2':6',2''-terpyridin-6-yl]benzene L². *N*-[2-Oxo-2-(2,2'-bipyridin-6-yl)ethyl]pyridinium iodide (1.0 g, 2.5 mmol), 2,6-bis(4-*tert*-butylcinnamoyl)benzene (0.56 g, 1.25 mmol) and ammonium acetate (4.5 g) were heated to reflux in acetic acid (15 cm³) for 8 h. A white precipitate was collected and recrystallized twice from toluene to give L² (0.73 g, 73%) (Found: C, 83.90; H, 6.10; N, 10.35. Calc. for C₅₆H₄₈N₆: C, 83.55; H, 6.00; N, 10.45%) ¹H NMR (270 Mz, CDCl₃): δ 1.42 (s, 18 H), 7.35 (dd, 2 H), 7.71 (t, 1 H), 7.72 (dd, 8 H), 7.89 (dt, 2 H), 8.01 (t, 2 H), 8.12 (d, 2 H), 8.33 (dd, 2 H), 8.50 (d, 2 H), 8.68 (d, 2 H), 8.72 (d, 2 H), 8.80 (d, 2 H), 8.85 (d, 2 H), and 9.02 (s, 1 H). Mass spectrum (EI): m/z 804 (*P*) and 727 (*P* – py).

[Cu₂L₂][PF₆]₄ 1 and [Cu₂L₂][PF₆]₄ 2. A suspension of copper(II) acetate (0.05 g, 0.27 mmol) and compound L¹ (0.154 g, 0.27 mmol) or L² (0.221 g, 0.27 mmol) in methanol (10 cm³) was refluxed for 30 min. The solution changed quickly from blue to green and L gradually disappeared. After filtering, the filtrate was treated with a saturated methanolic solution of NH₄PF₆. Green microcrystals in nearly quantitative yield were obtained. The complexes can be recrystallized by diffusion of diethyl ether into acetonitrile solutions; [Cu₂L₂][PF₆]₄ (Found: C, 48.10; H, 2.60; N, 9.40. Calc. for C₇₂H₄₈Cu₂F₂₄N₁₂P₄: C, 48.35; H, 2.70; N, 9.40%), UV/VIS (MeCN) λ_{max}/nm (ε/dm³ mol⁻¹ cm⁻¹) 225 (1.23 × 10⁵), 275 (7.79 × 10⁴), 308 (9.01 × 10⁵) and 337 (4.05 × 10⁴); [Cu₂L₂][PF₆]₄ (Found: C, 58.50; H, 4.15; N, 7.30. Calc. for C₁₁₂H₉₆Cu₂F₂₄N₁₂P₄: C, 58.05; H, 4.20; N, 7.25%); UV/VIS (MeCN) λ_{max}/nm (ε/dm³ mol⁻¹ cm⁻¹) 226 (1.58 × 10⁵), 263 (9.39 × 10⁴), 308 (1.00 × 10⁵), and 338 (5.44 × 10⁴).

[Ag₂L₂][PF₆]₂ 3 and [Ag₂L₂][PF₆]₂ 4. A suspension of silver acetate (0.05 g, 0.30 mmol) and compound L¹ (0.168 g, 0.30 mmol) or L² (0.241 g, 0.30 mmol) in methanol (10 cm³) was refluxed in the dark for 8 h. The solution was filtered and the filtrate treated with a saturated methanolic solution of NH₄PF₆. A yellowish solid was precipitated. The complex was purified by chromatography on a 10 × 300 mm alumina column with acetonitrile as the eluent. Pale yellow needles were obtained upon slow diffusion of diethyl ether into acetone solutions: [Ag₂L₂][PF₆]₂ (Found: C, 53.80; H, 2.95; N, 10.50. Calc. for C₇₂H₄₈Ag₂F₁₂N₁₂P₂: C, 54.50; H, 3.05; N, 10.60%); ¹H NMR (270 Mz, CD₃CN) δ 6.80 (dd, 4 H), 6.82 (m, 6 H), 7.12 (d, 4 H), 7.26 (d, 4 H), 7.50 (dt, 4 H), 7.53 (d, 4 H), 7.59 (d, 4 H), 7.63 (t, 4 H), 7.65 (d, 4 H), 7.75 (d, 4 H), 7.84 (t, 4 H) and 9.69 (s, 2 H); UV/VIS (MeCN), λ_{max}/nm (ε/dm³ mol⁻¹ cm⁻¹) 234 (1.06 × 10⁵), 286 (4.30 × 10⁴) and 313 (4.11 × 10⁴); [Ag₂L₂][PF₆]₂ Found: C, 63.35; H, 4.45; N, 7.90. Calc. for C₁₁₂H₉₆Ag₂F₁₂N₁₂P₂: C, 63.60; H, 4.55; N, 7.95%); ¹H NMR (270 Mz, CD₃CN) δ 1.44 (s, 36 H), 6.80 (t, 2 H), 6.82 (t, 4 H), 7.12 (dd, 4 H), 7.42 (m, 12 H), 7.68 (m, 32 H), 7.80

(t, 4 H) and 9.92 (s, 2 H); UV/VIS (MeCN) λ_{max}/nm (ε/dm³ mol⁻¹ cm⁻¹) 233 (1.32 × 10⁵), 274 (1.24 × 10⁵) and 313 (5.19 × 10⁴).

[Ru₂L²(terpy)₂][PF₆]₄ 5. A suspension of [Ru(terpy)Cl₃] (0.1 g, 0.23 mmol) and compound L² (0.09 g, 0.11 mmol) in degassed methanol (100 cm³) was refluxed for 48 h. The solution gradually turned orange. After filtering, the filtrate was treated with a saturated methanolic solution of NH₄PF₆ and allowed to stand at 0 °C overnight. A dark orange crystalline solid precipitated and was filtered off. Orange needles were obtained by diffusion of diethyl ether into acetonitrile solution (Found: C, 50.65; H, 3.25; N, 8.10. Calc. for C₈₆H₇₀F₂₄N₁₂P₄Ru₂: C, 50.30; H, 3.45; N, 8.20%) ¹H NMR (500 Mz, CD₃CN): δ 1.42 (s, 18 H), 5.75 (d, 2 H), 6.09 (d, 2 H), 6.27 (s, 1 H), 6.39 (t, 1 H), 6.84 (d, 2 H), 6.96 (t, 2 H), 7.10 (t, 2 H), 7.32 (d, 2 H), 7.39 (t, 2 H), 7.58 (d, 2 H), 7.67 (t, 2 H), 7.70 (t, 2 H), 7.74 (t, 2 H), 7.81 (d, 8 H), 7.85 (d, 2 H), 7.87 (d, 2 H), 8.09 (t, 2 H), 8.32 (d, 2 H), 8.33 (d, 2 H), 8.49 (d, 2 H), 8.50 (t, 2 H), 8.68 (d, 2 H), 8.89 (d, 2 H) and 9.11 (d, 2 H). UV/VIS spectral data (MeCN): λ_{max}/nm (ε/dm³ mol⁻¹ cm⁻¹) 232 (9.29 × 10⁴), 274 (9.07 × 10⁴), 312 (1.15 × 10⁵) and 481 (3.03 × 10⁴).

X-Ray crystallography

Crystal data. C₁₂₄H₁₁₄Cu₂F₂₄N₁₈P₄, 2·6MeCN, *M_r* = 2563.31, monoclinic, space group *C2/c*, *a* = 32.049(6), *b* = 12.27(2), *c* = 30.561(4) Å, β = 94.69(1)°, *U* = 11 981(3) Å³, *Z* = 4, *D_c* = 1.421 g cm⁻³, μ(Mo-Kα) = 4.397 cm⁻¹, crystal dimensions 0.05 × 0.20 × 0.35 mm, *F*(000) = 5278.

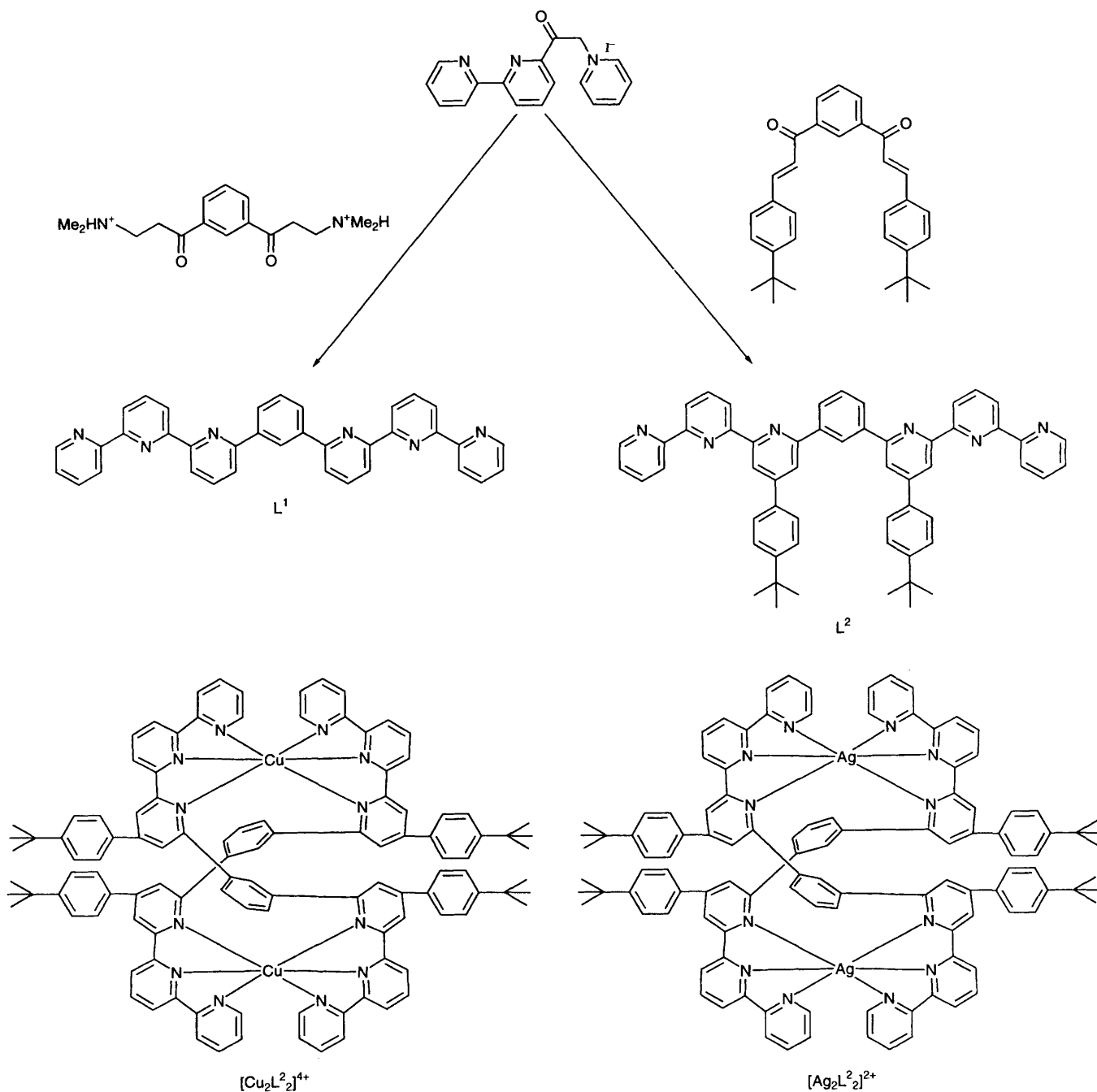
C₁₁₅H₁₀₂Ag₂F₁₂N₁₂OP₂, 4·Me₂CO, *M_r* = 2173.82, monoclinic, space group *C2/c*, *a* = 18.124(4) Å, *b* = 26.212(6) Å, *c* = 22.406(6) Å, β = 97.17(3)°, *U* = 10 561(4) Å³, *Z* = 4, *D_c* = 1.363 g cm⁻³, μ(Mo-Kα) = 4.766 cm⁻¹, crystal dimensions 0.20 × 0.25 × 0.50 mm, *F*(000) = 4442.

The X-ray diffraction data were collected on an Enraf-Nonius CAD-4 four-circle diffractometer (graphite-monochromatized Mo-Kα radiation, λ = 0.7107 Å) at National Taiwan University using the ω–2θ scan mode with 2θ_{max} = 45.0°. The data were corrected for absorption. All data reduction and structure refinement were performed using the NRCC-SDP-VAX packages.¹⁵ The structures were solved by the Patterson method and refined by least squares. The weight scheme was *w*⁻¹ = σ²(*F*). For complex 2 the last least-squares cycle was calculated with 145 atoms, 695 parameters and 2322 reflections (|*I*_o| > 2.0σ|*I*_o|) out of 7828 unique reflections giving *R* = 0.063, *R'* = 0.060, goodness of fit = 2.00. The final Fourier-difference map showed residual extrema in the range of –0.380 to 0.450 e Å⁻³. For complex 4, the last least-squares cycle was calculated with 123 atoms, 632 parameters and 2444 reflections (|*I*_o| > 2.0σ|*I*_o|) out of 6894 unique reflections giving *R* = 0.065, *R'* = 0.068, goodness of fit = 2.02. The final Fourier-difference map showed residual extrema in the range of –0.380 to 0.680 e Å⁻³.

Complete atomic coordinates, thermal parameters and bond lengths and angles have been deposited at the Cambridge Crystallographic Data Centre. See Instructions for Authors, *J. Chem. Soc., Dalton Trans.*, 1996, Issue 1.

Results and Discussion

The synthetic routes to L¹ and L² and schematic drawings of the double helical metal complexes of L² are given in Scheme 1. The synthetic strategy follows the procedures developed by Kröhnke¹⁶ and Constable *et al.*¹¹ The higher members of oligopyridines usually have low solubility in common organic solvents. Introduction of the 1,3-phenylene spacer would enhance the solubility of these ligands due to the irregularity in the stack of pyridine rings. Thus, although L¹, and



Scheme 1 Synthetic routes of L^1 and L^2

2,2':6',2'':6'',2''':6''',2''''':6''''',2''''''-septapyridine^{16,17} have the same number of aromatic rings, the former has a much higher solubility in common organic solvents. However, the product yield of L^1 is low and it is difficult to obtain pure. Insertion of a 4-*tert*-butylphenyl group on the pyridine backbone gives L^2 , which has a higher solubility than L^1 (ref. 18) and is more easily purified. Moreover, both L^1 and L^2 are anticipated to have the same bonding and electrochemical properties, thus making the latter more attractive.

Treatment of compounds L^1 and L^2 with $M(O_2CMe)_n$ ($M = Cu^{II}$, $n = 2$; $M = Ag^I$, $n = 1$) in methanol would give double helical metal complexes. The reactions are self-assembling in nature as the products are unaffected by the initial metal:ligand ratio. The 1H NMR spectrum of $[Ag_2L^1_2]^{2+}$ in CD_3CN at room temperature is shown in Fig. 1. Based on it the silver complex is diamagnetic and the two L^1 ligands are equivalent and symmetrical about the phenylene spacers. However, as will be mentioned later, the crystal structure of the related $[Ag_2L^2_2]^{2+}$ complex shows that L^2 is

not symmetrical about the phenylene spacer. In view of this finding, the 1H NMR spectrum of $[Ag_2L^1_2]^{2+}$ was recorded at $-80^\circ C$ to see if there is any fluxional behaviour. It has been found that all the proton signals are broadened at $-80^\circ C$ suggesting that the complexes are undergoing some changes with rates comparable to the NMR time-scale. This is consistent with a rapid exchange reaction involving the approach to and departure of the pyridyl donors N(1) and N(6) (see Fig. 4 for atom numbering) from the co-ordination sphere of the silver(I) ions. Like $[Ag_2L_2]^{2+}$ [$L = 1,3$ -bis-(2,2'-bipyridin-6-yl)benzene],¹¹ most of the aromatic protons of $[Ag_2L^1_2]^{2+}$ and $[Ag_2L^2_2]^{2+}$ occur in the region with $\delta < 8$. This is attributed to the anisotropy arising from π - π stacking interactions. Owing to the geometric requirements of forming double helicates, the 1,3-phenylene spacers point towards each other. This leads to a downfield shift of the proton H_a (for numbering see Fig. 1), which is the proton of the phenylene spacer in between the two interannular bonds, with δ 9.69 for $[Ag_2L^1_2]^{2+}$ and δ 9.92 for $[Ag_2L^2_2]^{2+}$. Unlike $[Ag_2L^1_2]^{2+}$,

the ^1H NMR spectrum of $[\text{Ag}_2\text{L}^2_2]^{2+}$ shows serious overlapping of ^1H signals within the region δ 7.6–7.8.

Two equivalents of $[\text{Ru}(\text{terpy})\text{Cl}_3]$ and 1 equivalent of L^2 in methanol gave $[\text{Ru}_2\text{L}^2(\text{terpy})_2]^{4+}$. We suggest that the reaction proceeds through the reduction of Ru^{III} to Ru^{II} in methanol. The product is the first reported single helical ruthenium complex, and shows a well resolved ^1H NMR spectrum in CD_3CN at room temperature. As illustrated in Fig. 2 ^1H - ^1H correlation spectroscopy (COSY) shows 25 non-equivalent signals that are due to the 52 aromatic protons. It can be inferred from the spectrum that (i) the ratio of L^2 to terpy is 1:2, and (ii) the co-ordinated L^2 has two-fold symmetry but the two terpyridines do not. The NMR data are consistent with a binuclear single helical model having a two-fold axis.

The crystal structures of $[\text{Ag}_2\text{L}^2_2][\text{PF}_6]_2 \cdot \text{Me}_2\text{CO}$ and $[\text{Cu}_2\text{L}^2_2][\text{PF}_6]_4 \cdot 6\text{MeCN}$ have been determined. However, due to the low diffractivity of the crystals, the numbers of observed reflections that could be used in the refinements are low in each case. Nevertheless, the double helical structures have been confirmed, and perspective views of the complex cations are shown in Figs. 3 and 4. The crystal structure of $[\text{Ag}_2\text{L}^2_2]^{2+}$ reveals a double helical bimetallic silver(I) complex. Each Ag^{I} adopts an irregular five co-ordination. The $[\text{Cu}_2\text{L}^2_2]^{4+}$ cation adopts a distorted-octahedral co-ordination geometry. The two 4-(4-*tert*-butylphenyl)-2,2':6',2''-terpyridin-6-yl groups are in a *mer* configuration. So far, we have not been able to obtain

crystals of $[\text{Ru}_2\text{L}^2(\text{terpy})_2][\text{PF}_6]_4$ suitable for X-ray crystal analysis.

Electrospray mass spectrometry (ESMS) is a good method for examining ionic species in solution and has wide applications in inorganic and organometallic chemistry. In this work the complexes $[\text{Cu}_2\text{L}^2_2][\text{PF}_6]_4$, $[\text{Ag}_2\text{L}^2_2][\text{PF}_6]_2$ and $[\text{Ru}_2\text{L}^2(\text{terpy})_2][\text{PF}_6]_4$ were examined. Table 1 lists the m/z values of the principal ions and the ES mass spectra of $[\text{Ag}_2\text{L}^2_2][\text{PF}_6]_2$ and $[\text{Ru}_2\text{L}^2(\text{terpy})_2][\text{PF}_6]_4$ are shown in Fig. 5. In all cases, the agreement between experimental and calculated isotopic mass distribution is excellent. For $[\text{Cu}_2\text{L}^2_2][\text{PF}_6]_4$ and $[\text{Ru}_2\text{L}^2(\text{terpy})_2][\text{PF}_6]_4$ the most abundant ions in acetone solutions are the $[\text{Cu}_2\text{L}^2_2(\text{PF}_6)]^{3+}$ and $[\text{Ru}_2\text{L}^2(\text{terpy})_2(\text{PF}_6)]^{3+}$ ions. However, for $[\text{Ag}_2\text{L}^2_2][\text{PF}_6]_2$, the dominant ion is $[\text{Ag}_2\text{L}^2_2]^{2+}$ and there is no other higher

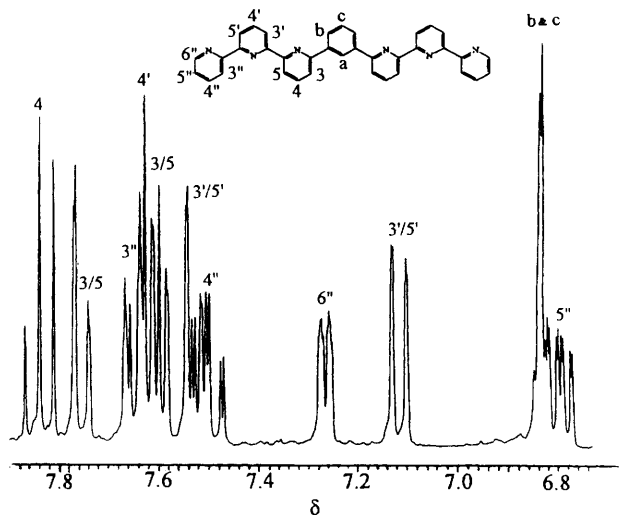


Fig. 1 Proton NMR spectrum of $[\text{Ag}_2\text{L}^2_2][\text{PF}_6]_2$ in CD_3CN

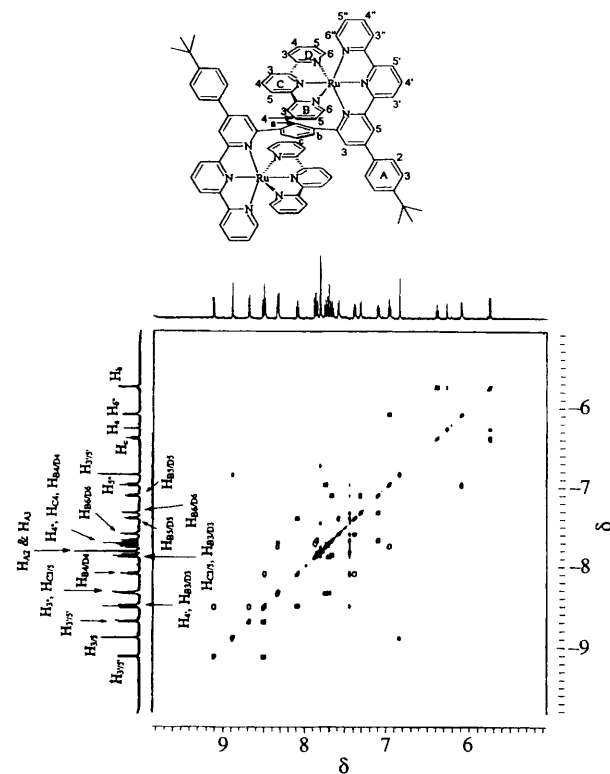


Fig. 2 The ^1H - ^1H COSY spectrum of $[\text{Ru}_2\text{L}^2(\text{terpy})_2][\text{PF}_6]_4$ in CD_3CN showing the proton numbering scheme

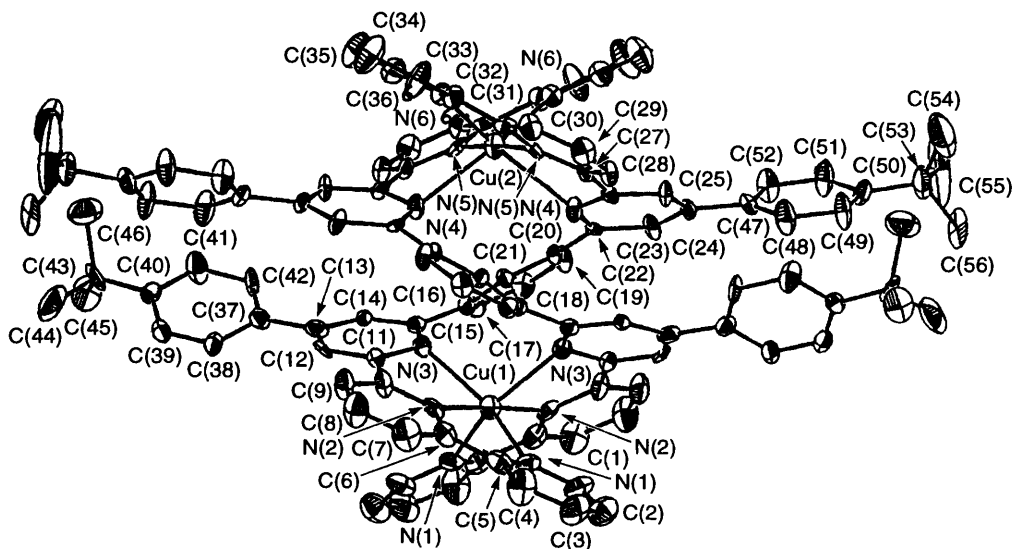


Fig. 3 Perspective drawing of the complex cation $[\text{Cu}_2\text{L}^2_2]^{4+}$

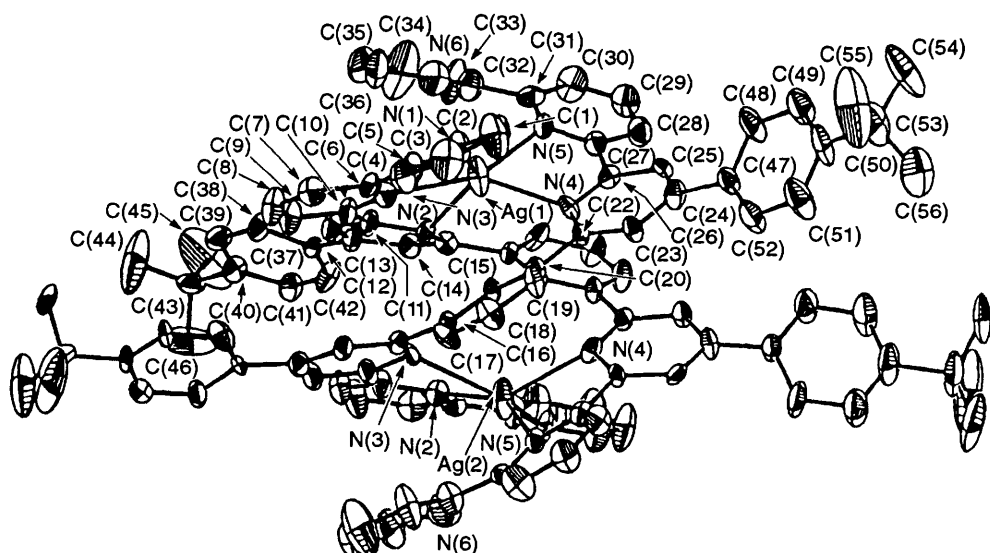


Fig. 4 Perspective drawing of the complex cation $[\text{Ag}_2\text{L}_2]^{2+}$

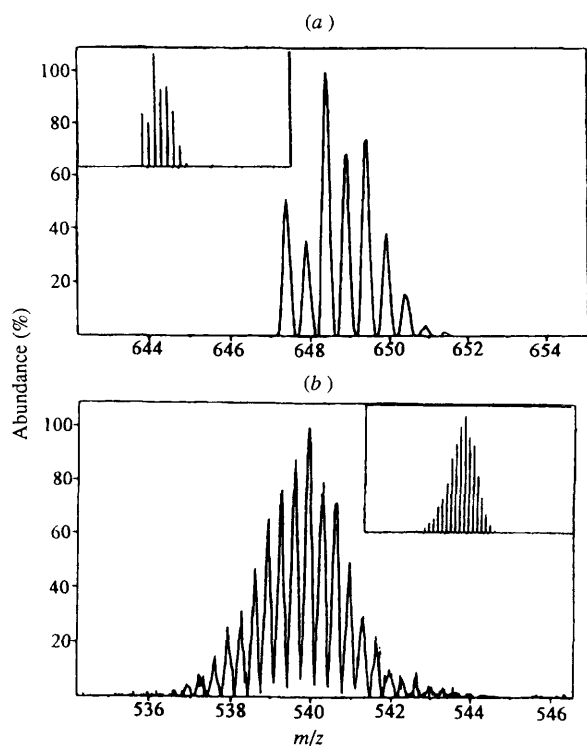


Fig. 5 The most abundant ions in the ES mass spectra of (a) $[\text{Ag}_2\text{L}_2][\text{PF}_6]_2$ and (b) $[\text{Ru}_2\text{L}_2(\text{terpy})_2][\text{PF}_6]_4$. The simulated spectra are shown as insets

Table 1 Principal ions in the ES mass spectra of the complexes

Complex	Principal ions (m/z , relative abundance in %)
$[\text{Cu}_2\text{L}_2][\text{PF}_6]_4$	$[\text{Cu}_2\text{L}_2]^{4+}$ (434.3, 53) $[\text{Cu}_2\text{L}_2(\text{PF}_6)]^{3+}$ (625.7, 100) $[\text{Cu}_2\text{L}_2(\text{PF}_6)_2]^{2+}$ (1013.9, 40)
$[\text{Ag}_2\text{L}_2][\text{PF}_6]_2$	$[\text{Ag}_2\text{L}_2]^{2+}$ (648.4, 100) $[\text{Ag}_2\text{L}_2(\text{PF}_6)]^+$ (1442.0, 34)
$[\text{Ru}_2\text{L}_2(\text{terpy})_2][\text{PF}_6]_4$	$[\text{Ru}_2\text{L}_2(\text{terpy})_2]^{4+}$ (368.7, 63) $[\text{Ru}_2\text{L}_2(\text{terpy})_2(\text{PF}_6)]^{3+}$ (539.8, 100) $[\text{Ru}_2\text{L}_2(\text{terpy})_2(\text{PF}_6)_2]^{2+}$ (882.2, 47)

charged species. This indicates a subtle balance of the charge density of the ionic species in the solvent. The ES mass spectra provide an excellent demonstration of the existence of the

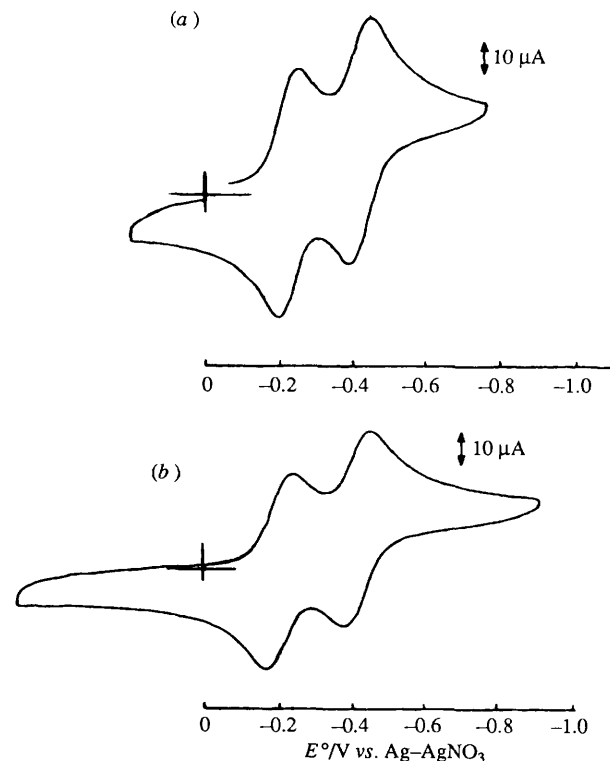


Fig. 6 Cyclic voltammograms of (a) $[\text{Cu}_2\text{L}_2][\text{PF}_6]_4$ and (b) $[\text{Cu}_2\text{L}_2][\text{PF}_6]_4$

Table 2 Values of E_1 for the redox couples of the complexes

Complex	E_1/V ($\Delta E_p/\text{mV}$)
$[\text{Cu}_2\text{L}_2][\text{PF}_6]_4$	-0.22(60), -0.41(60)
$[\text{Cu}_2\text{L}_2][\text{PF}_6]_4$	-0.21(80), -0.42(80), -2.14 ^a
$[\text{Ag}_2\text{L}_2][\text{PF}_6]_2$	+0.81(50), +0.94(50)
$[\text{Ag}_2\text{L}_2][\text{PF}_6]_2$	+0.79(80), +0.95(80), -1.73 ^a
$[\text{Ru}_2\text{L}_2(\text{terpy})_2][\text{PF}_6]_4$	+0.98(80), -1.56(80), -1.88 ^b , -2.36 ^a

^a Irreversible. ^b Quasi-reversible.

double helical bimetallic silver(I) and copper(II) and single helical ruthenium(II) complexes.¹⁹

All five complexes display intriguing electrochemistry. The electrochemical data are summarized in Table 2 and cyclic voltammograms of $[\text{Cu}_2\text{L}_2][\text{PF}_6]_4$ and $[\text{Cu}_2\text{L}_2][\text{PF}_6]_4$

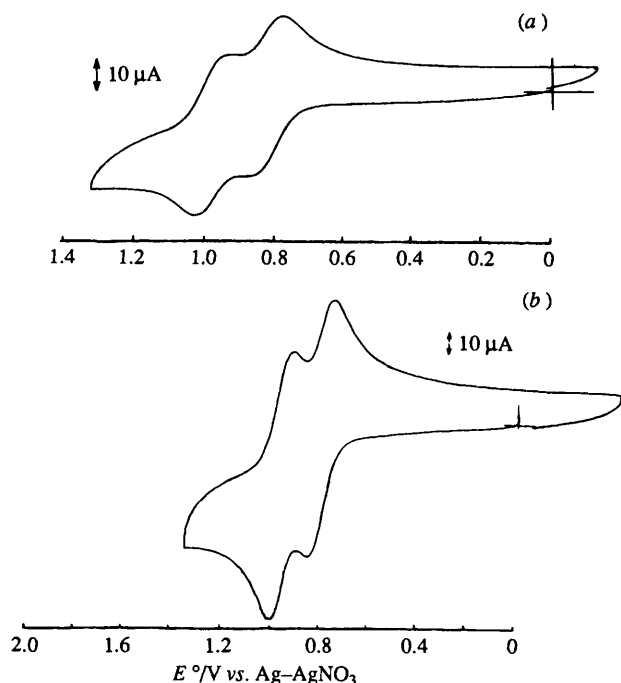


Fig. 7 Cyclic voltammograms of (a) $[\text{Ag}_2\text{L}^{1.2}][\text{PF}_6]_2$ and (b) $[\text{Ag}_2\text{L}^{2.2}][\text{PF}_6]_2$

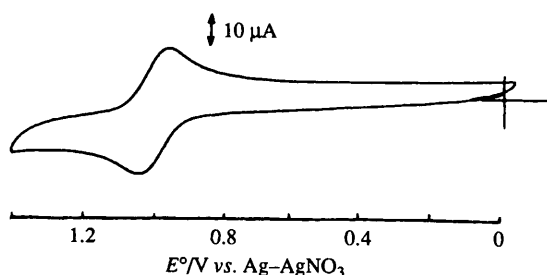


Fig. 8 Cyclic voltammogram of $[\text{Ru}_2\text{L}^2(\text{terpy})_2][\text{PF}_6]_4$

measured in acetonitrile solutions are shown in Fig. 6. In the potential region from 0.0 to +1.9 V there is no oxidation couple. For $[\text{Cu}_2\text{L}^{1.2}]^{4+}$ two reduction couples are observed at E_1 values of -0.22 and -0.41 V. Both are reversible and have a peak-to-peak separation of ca. 60 mV and a current ratio $i_{pa}/i_{pc} > 0.9:1$ at scan rates from 20 to 100 mV s^{-1} . By constant-potential electrolysis, both couples are found to be one electron in nature. They are tentatively assigned as $\text{Cu}^{\text{II}}\text{Cu}^{\text{II}}-\text{Cu}^{\text{I}}\text{Cu}^{\text{II}}$ and $\text{Cu}^{\text{I}}\text{Cu}^{\text{II}}-\text{Cu}^{\text{I}}\text{Cu}^{\text{I}}$. The 190 mV difference in E_1 value between the two couples indicates a substantial electronic coupling between the two metal centres^{4b} through the phenylene spacer. In other words, the bimetallic system does not behave as two discrete $[\text{Cu}(\text{terpy})_2]^{2+}$ units. The voltammetric cycles are stable upon several scans. This is different from the related $[\text{Cu}_2(\text{mtsexpy})_2][\text{PF}_6]_2$ ^{4b} [mtsexpy = 4',4''-bis(methylthio)-2,2':6',2'':6''',2'''-sexipyridine] complex which undergoes a geometrical change after reduction. For $[\text{Cu}_2\text{L}^2][\text{PF}_6]_4$ two similar reduction couples have been found at E_1 values of -0.21 and -0.42 V. In addition, a ligand-centred reduction has been observed at -2.14 V.

Neither $[\text{Ag}_2\text{L}^{1.2}][\text{PF}_6]_2$ nor $[\text{Ag}_2\text{L}^{2.2}][\text{PF}_6]_2$ has a voltammetric response in the potential region 0.0 to -1.9 V except for the ligand-based reduction at -1.73 V for the latter. The voltammograms are shown in Fig. 7. Both silver complexes show two reversible oxidation couples corresponding to the oxidations $\text{Ag}^{\text{I}}\text{Ag}^{\text{I}}$ to $\text{Ag}^{\text{II}}\text{Ag}^{\text{I}}$ and $\text{Ag}^{\text{II}}\text{Ag}^{\text{I}}$ to $\text{Ag}^{\text{II}}\text{Ag}^{\text{II}}$. The E_1 values are +0.81, +0.94 V for $[\text{Ag}_2\text{L}^{1.2}][\text{PF}_6]_2$ and +0.79, +0.95 V for $[\text{Ag}_2\text{L}^{2.2}][\text{PF}_6]_2$. Like the copper complexes, there is a high degree of electronic coupling which is reflected by the large potential differences between the two oxidation couples.

The voltammograms are stable upon repetitive scans suggesting that the geometrical change accompanying oxidation of Ag^{I} to Ag^{II} is small.

The complex $[\text{Ru}_2\text{L}^2(\text{terpy})_2][\text{PF}_6]_4$ behaves quite differently from the four double helical complexes. As shown in Fig. 8 it displays only one reversible oxidation couple at +0.98 V corresponding to the two-electron oxidation $\text{Ru}^{\text{II}}\text{Ru}^{\text{II}}-\text{Ru}^{\text{III}}-\text{Ru}^{\text{III}}$. The assignment is based on the related $[\text{Ru}(\text{terpy})_2][\text{ClO}_4]_2$ which has a metal-centred oxidation at +1.18 V.²⁰ There are three ligand-centred reductions at -1.56, -1.88 and -2.36 V.

Acknowledgements

We acknowledge support from The University of Hong Kong, The Hong Kong Research Grants Council and the Croucher Foundation.

References

- 1 E. C. Constable, M. G. B. Drew and M. D. Ward, *J. Chem. Soc., Chem. Commun.*, 1987, 1600; M. Barley, E. C. Constable, S. A. Corr, R. C. S. McQueen, J. C. Nutkins, M. D. Ward and M. G. B. Drew, *J. Chem. Soc., Dalton Trans.*, 1988, 2655; E. C. Constable, M. D. Ward, M. G. B. Drew and G. A. Forsyth, *Polyhedron*, 1989, **8**, 2551; E. C. Constable, S. M. Elder, P. R. Raithby and M. D. Ward, *Polyhedron*, 1991, **10**, 1395; E. C. Constable, J. V. Walker, D. A. Tocher and M. A. M. Daniels, *J. Chem. Soc., Chem. Commun.*, 1992, 768; E. C. Constable, M. A. M. Daniels, M. G. B. Drew, D. A. Tocher, J. V. Walker and P. D. Wood, *J. Chem. Soc., Dalton Trans.*, 1993, 1947.
- 2 E. C. Constable, M. G. B. Drew, G. Forsyth and M. D. Ward, *J. Chem. Soc., Chem. Commun.*, 1988, 1450.
- 3 E. C. Constable, S. M. Elder, J. Healy and M. D. Ward, *J. Am. Chem. Soc.*, 1990, **112**, 4590; E. C. Constable and J. V. Walker, *J. Chem. Soc., Chem. Commun.*, 1992, 884.
- 4 (a) K. T. Potts, K. A. G. Raiford and M. Keshavarz-K, *J. Am. Chem. Soc.*, 1993, **115**, 2793; (b) K. T. Potts, M. Keshavarz-K, F. S. Tham, H. D. Abruna and C. Arana, *Inorg. Chem.*, 1993, **32**, 4436.
- 5 E. C. Constable and M. D. Ward, *J. Am. Chem. Soc.*, 1990, **112**, 1256.
- 6 E. C. Constable, M. D. Ward and D. A. Tocher, *J. Chem. Soc., Dalton Trans.*, 1991, 1675.
- 7 E. C. Constable and R. Chotalia, *J. Chem. Soc., Chem. Commun.*, 1992, 64.
- 8 E. C. Constable, R. Chotalia and D. A. Tocher, *J. Chem. Soc., Chem. Commun.*, 1992, 771.
- 9 M. T. Youinou, R. Ziessel and J.-M. Lehn, *Inorg. Chem.*, 1991, **30**, 2144; Y. Yao, M. W. Perkovic, D. P. Rillema and C. Woods, *Inorg. Chem.*, 1992, **31**, 3956; A. Juris and R. Ziessel, *Inorg. Chim. Acta*, 1994, **225**, 251.
- 10 J.-M. Lehn and A. Rigault, *Angew. Chem., Int. Ed. Engl.*, 1988, **27**, 1095; A. Pfeil and J.-M. Lehn, *J. Chem. Soc., Chem. Commun.*, 1992, 838.
- 11 E. C. Constable, M. J. Hannon and D. A. Tocher, *J. Chem. Soc., Dalton Trans.*, 1993, 1883.
- 12 E. C. Constable, M. J. Hannon and D. R. Smith, *Tetrahedron Lett.*, 1994, **35**, 6657.
- 13 W. E. Smith, *J. Org. Chem.*, 1972, **37**, 3973.
- 14 P. A. Adcock, R. F. Keene, R. S. Smythe and M. R. Snow, *Inorg. Chem.*, 1984, **23**, 2336.
- 15 E. J. Gabe, Y. Le Page, J. P. Charland, F. L. Lee and P. S. White, *J. Appl. Crystallogr.*, 1989, **22**, 384.
- 16 F. Kröhnke, *Synthesis*, 1976, 1.
- 17 C. M. Che, unpublished work.
- 18 E. C. Constable, P. Harverson, D. R. Smith and L. A. Whell, *Tetrahedron*, 1994, **50**, 7799.
- 19 R. Colton and J. C. Traeger, *Inorg. Chim. Acta*, 1992, **201**, 153; R. Colton, J. C. Traeger and J. Harvey, *J. Org. Mass Spectrom.*, 1992, **27**, 1030; R. Colton, V. Tedesco and J. C. Traeger, *Inorg. Chem.*, 1992, **31**, 3865; I. Ahmed, A. M. Bond, R. Colton, M. Jurcevic, J. C. Traeger and J. N. Walter, *J. Organomet. Chem.*, 1993, **455**, 283; A. J. Canty, P. R. Traill, R. Colton and I. M. Thomas, *Inorg. Chim. Acta*, 1993, **210**, 91.
- 20 D. E. Morris, K. W. Hanck and M. K. DeArmond, *J. Electroanal. Chem., Interfacial Electrochem.*, 1983, **149**, 115.

Received 5th December 1995, Paper 5/07915B